Ceramics-Silikáty 63 (2), 213-222 (2019)
www.ceramics-silikaty.cz doi: 10.13168/cs.2019.0013

MICROSTRUCTURE AND MECHANICAL PROPERTIES OF ANNEALED WC/C COATINGS DEPOSITED WITH DIFFERENT GAS MIXTURES IN AN RFMS PROCESS

PETER HORŇÁK*, **, #DANIEL KOTTFER***, LUKASZ KACZMAREK****, KAROL KYZIOL*****, JÁN VAVRO*, MAREK KLICH****, JOZEF TREBUŇA***, MAREK VRABEĽ***, MÁRIA FRANKOVÁ***

*Alexander Dubček University of Trenčín, Faculty of Industrial Technologies, I. Krasku 491/30, 020 01 Púchov, Slovakia
**Slovak Academy of Sciences, Institute of Materials Research, Watsonova 47, 040 01 Košice, Slovakia
***Technical University of Košice, Faculty of Mechanical Engineering, Mäsiarska 74, 040 01 Košice, Slovakia
****Lodz University of Technology, Institute of Materials Science and Engineering, 1/15 Stefanowskiego Str., 90-924 Łódź, Poland
*****AGH University of Science and Technology, Faculty of Materials Science and Ceramics, A. Mickiewicza 30 Av., 30-059, Kraków, Poland

#E-mail: daniel.kottfer@tuke.sk

Submitted November 16, 2018; accepted February 17, 2019

Keywords: WC/C coating, RF magnetron sputtering, Annealing, Mechanical properties, Coefficient of friction

The optimised indented hardness (H_{IT}) of WC/C coatings deposited using an RF magnetron sputtering technique in relation to the vacuum chamber pressure and bias is presented in this paper. Based on the investigation, the maximal values of hardness (ca. 22.3 GPa) and Young's modulus (ca. 298 GPa) are shown. Besides the hardness and Young's modulus values, the minimal value of the coefficient of friction (COF) ca. 0.29 was obtained. WC/C coatings were deposited with and without N_2 and N_2 + SiH_4 (in a gas mixture) and they were subsequently annealed at 200 °C, 500 °C and 800 °C. Finally, they were evaluated from the aspect of H_{IT}, E_{IT}, COF and morphology as well as from the structural composition of the WC/C coatings before and after annealing.

INTRODUCTION

In materials engineering, the highest melting temperature is the typical feature of tungsten (W) and silicon (Si), which are used in many industrial operations for the deposition of hard coatings in the form of silicon carbide (SiC) [1], tungsten metal nitride [2] and tungsten carbide (WC). WC has an excellent combination of properties, such as high hardness, Young's modulus, corrosion and oxidation resistance. On the other hand, it has a low friction coefficient. The WC coating can be deposited on the substrate material by magnetron sputtering, including a direct current magnetron sputtering (DC MS) technique [3-13] and a radio frequency magnetron sputtering (RF MS) technique [14-24]. Moreover, WC coatings can be deposited with a low-pressure and low-temperature plasma system, where tungsten carbonyl is used as a precursor [25-29] and it enables the temperature to decrease near to 300 °C [19]. It should be pointed out that there is also high target utilisation sputtering (HiTUS) [30], which belongs among the effective techniques of sputtering.

Abdelouahdi et *al.* [14] measured WC/C coatings deposited via the RF MS technique. They changed the methane concentrations. Estéve et *al.* [15] evaluated WC/C coatings deposited with methane concentrations from 7 % up to 31 %. The coatings deposited from 17 % up to 24 % CH_4 in the gas mixtures showed the highest hardness, in the range 24 ÷ 26 GPa. In addition, Rincón et *al.* [16] deposited WC/C coatings with CH_4 added gas. Abad et *al.* [17] and El Mrabet et *al.* [18] deposited WC/C nanostructured coatings with carbon contents ranging from 30 % up to 70 at. % on M2 steel substrates by magnetron sputtering of WC and graphite targets in argon. They obtained H_{IT} and FC from 16 up to 40 GPa and from 0.19 up to 0.81, respectively. Also, based on their research, they carried-out a comparative analysis of hardness, stress, COF and C content in the WC/C coatings. Czyzniewski [19] also deposited WC and nanocomposite WC/a-C:H coatings, using pulsed reactive magnetron sputtering of a tungsten target under an argon-acetylene atmosphere on steel substrates held at a temperature below 150 °C (423 K). The obtained results of the evaluated properties and selected technological parameters for the coatings deposition are shown in Table 1. Besides the technological parameters, the temperature of the sample surface, the target-to-substrate distance (the distance of the target to the coated surface) and the magnetron power were variable. In order to influence the properties of the WC/C coatings, H_2 [20] and methane (CH_4) [14-16, 19] are the representatives of the gases, which are commonly used in the deposition process. The change in CH_4 flow was also involved in the investigation process because of its effect on the

mechanical WC/C coating properties. In relation to the investigation of the WC/C coatings deposition, both N_2 gas and a mixture of $N_2 + SiH_4$ were used in the case of the RF magnetron sputtering process, because there are not any other effective gases or mixtures of gases to be used as additives for the mentioned deposition based on the given sputtering process. Also, there is lack information about such description phenomena in literature.

Due to that, the goal of this work is to optimise the technological parameters for the WC/C coating deposition using the RF magnetron sputtering technique in relation to the maximal hardness. The next goal is to investigate the effect of the temperature on the thermal stability, hardness, Young's modulus and COF of the WC/C coatings with and without the added gases, such as N_2 and $N_2 + SiH_4$. The obtained results are compared with the values reported by the above-mentioned authors.

EXPERIMENTAL

The preparation of the samples included the selection of C45 construction or structural steel, the chemical composition (wt. %) of which was in accordance with the Slovak Technical Standards (STN 412050): 0.42 ÷ 0.50 % C, max. 0.40 % Si, 0.50 ÷ 0.80 % Mn, max. 0.40 % Cr, max. 0.10 % Mo, max. 0.40 % Ni, max. 0.035 % P, max. 0.35 % S. The samples were made with wire electrical discharge machining (WEDM) from bars of circular cross-section profiles with diameters of 50 and 25 mm. Function surfaces have been machined to the thickness of 3 ± 0.05 mm. Then, the substrate samples were heated to 860 °C, quenched in oil and subsequently, they were annealed at 200 °C. After the given heat treatment, the substrate samples were polished with diamond polishing pastes which had different grit sizes, such as 15 μm, 9 μm and 3 μm, respectively. Finally, in order to have a smooth surface, the samples were polished with the diamond paste with grit size of 1 μm. Based on the polishing procedure hereinbefore, the resulting roughness of the substrate sample surfaces (R_a) was approximately 12 nm and it was measured using a confocal Plu Neox microscope (Sensofar, Spain Veeco, USA). Si substrates with thickness of 1.0 mm were used to study the high temperature effect on the oxide resistance of the WC/C coatings deposited using the RF magnetron sputtering (RF MS) technique. Before the deposition, the substrate samples were cleaned ultrasonically in acetone for 10 minutes. After placement in a vacuum chamber and subsequently ensuring the required yield pressure, the substrate samples were cleaned in an Ar glow discharge. The parameters of the cleaning process were: pressure (2 Pa), bias of the holder – $U_b \approx$ -5 kV, current density to the substrate samples (1 $mA \cdot cm^{-2}$) and the time of cleaning (15 minutes). In addition, Ar with a flow of 65 $cm^3 \cdot min^{-1}$ was blown into the vacuum chamber. After the cleaning procedure and ensuring the required yield pressure, which vas 10^{-3} Pa, the process of the WC/C coatings deposition on the substrate samples was performed.

Using the RF magnetron sputtering method [29], the operating pressure in the range from 0.1 Pa up to 2.0 Pa was used in the process of the WC/C coatings preparation. In the case of the PVD method, the presence of the carrier gas is required in order to create the glow discharge for emitting the target atoms. Relating to the experiment presented in this paper, argon (Ar) with a purity of 99.999 % was used as a carrier gas and the WC targets with a purity of 97 % and diameter of 90 mm were used as the source (cathode) material determined for the deposition. The target-to-substrate distance was kept constant and it was 100 mm. The negative bias was in the range from 0 V up to -80 V. During the experiment, the reactive additives, such as N_2 or N_2+SiH_4 were also used as doping agents.

After the deposition of the WC/C coatings, the annealing of the given samples was performed without any protective atmosphere in an electric furnace at 200 °C, 500 °C and 800 °C. The samples were held at each temperature for 1 hour and were subsequently left to be cooled freely to room temperature (RT).

The instrumented indentation hardness (H_{IT}) and indentation modulus (E_{IT}) were only measured after the annealing process at 200 °C. The H_{IT} and E_{IT} of the steel samples with coating were investigated with the utilisation of a nanoindentation tester (NHT), CSM Instruments, Switzerland. The prespecified parameters and testing conditions were as follows: a sinus mode with amplitude of 1 mN, the indentation load in the range from 20 mN to 60 mN, a frequency of 15 Hz.

Table 1. The selected published technological parameters for the deposition of WC/C RFMS coatings and some of their mechanical and tribological properties.

COF	Pressure (Pa)	Temperature (°C)	E_{IT} (GPa)	H_{IT} (GPa)	Ref.
0.1	0.25	150	–	13 – 22	14
–	10^{-4}	320	–	24 – 26	15
0.12 and 0.39	–	–	285 and 292	18.5 – 19.5	16
0.19 – 0.81	3×10^{-4}	150 – 200	270 – 520	16 – 40	17
–	–	–	–	–	18
–	2×10^{-3}	150	–	15 – 32	19

Each sample was subjected to 2 × 10 indentations. The curves of the extreme course were excluded from the analysis. The H_{IT} and E_{IT} values were calculated from the average maximum values, which were obtained from the indentation curves for each sample.

The friction coefficient of the WC/C coatings, which were deposited on the steel substrate samples, was measured with the ball-on-disc method, using a tribometer (HTT), CSM Instruments, Switzerland. The normal loading of 0.5 N and RT represent the predetermined parameters. The testing procedure was based on the indentation of a 100Cr6 steel ball with diameter of 6 mm, while the rotation speed of the samples was 10 $cm \cdot s^{-1}$ and the wear track varied from 50 to 200 m. The COF and the depth of the penetration were recorded continuously in dependence on time, the number of revolutions and the total length of the track. The wear of the evaluated coatings as well as their 100Cr6 steel ball counterpart was not subjected to the evaluation.

The COF of WC/C coatings on the Si substrate was measured with a fretting method, using a nanotribometer (NTR2), CSM Instruments, Switzerland, where the indentation loading was 0.5 N at RT. The 100Cr6 steel ball with diameter of 2 mm was used for the testing procedure. A frequency of 10 Hz, a wear track of 50 m and an amplitude of 3.2 mm represented the other predetermined parameters of the given testing procedure.

The surface morphology and microstructures of the coatings were evaluated by a JEOL 7000F scanning electron microscope (the SEM method). The thickness was evaluated from the as in-depth of the concentration of the GDOES profile. The chemical composition was determined in order to specify the approximate coating thickness for determining the loading force in the case of the H_{IT} measurement

The phase content of the WC/C coatings was measured by X-ray diffraction analysis, using an X´Pert PRO Philips with high-speed linear detector (X´Celerator) in a Bragg-Brentano para-focusing arrangement with an angular correlation of θ/2θ. A copper source was used (I = 40 kV, U = 50 mA) with the characteristic $CuK\alpha_{1,2}$ the X-rays and corresponding wavelength of 1.54 Å. The X-ray diffraction patterns were measured in the range from 10° up to 100° with a step size of 0.033°. The qualitative analysis was undertaken in the CMPR software – a powder diffraction toolkit [29] and evaluation was performed by comparison with the ICDD Powder Diffraction File (PDF-2) database.

The thickness of the evaluated coatings was determined indirectly using the GDOES method (Glow Discharge Optical Emission Spectroscopy) on the GDS-750 apparatus. This method is used for the qualitative and quantitative determination of metallic and non-metallic elements through a cross section of applied coatings up to a depth of 0.1 mm of the investigated material. From the concentration profile, it is possible to approximately deduct the coating thickness as well.

RESULTS AND DISCUSSION

Firstly, the deposition pressure with reference to the coating with the maximum hardness was determined. The effect of the deposition pressure on the indentation hardness as well as modulus can be seen in Figure 1. In the case of the coating deposition, the yield values of the deposition pressure in the vacuum chamber were 0.8 Pa and 2 Pa. When the deposition pressure was not in the interval ranging from 0.8 Pa up to 2 Pa, the deposition process could not be performed in a controlled way. In order to optimise the deposition process, the values of the deposition pressures were: 0.8, 1.0, 1.2, 1.5 and 2.0 Pa, respectively. The negative bias (U_b) of the sample holder was 0 V during the deposition process. Based on the optimisation results with reference to the coating with the maximum hardness, the optimum deposition pressure was 1.2 Pa for the WC/C coatings deposited with RF MS [29].

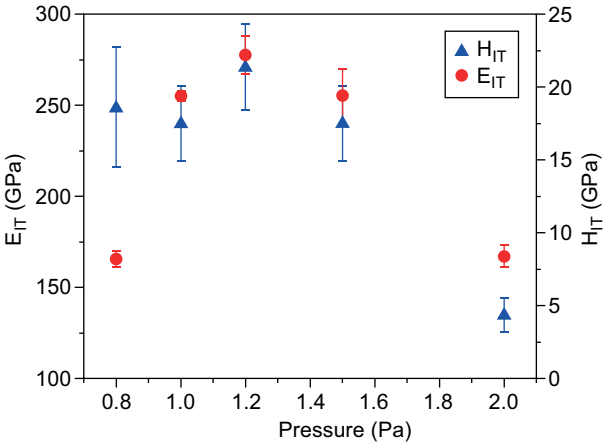

Figure 1. The surface H_{IT} and E_{IT} of the tested samples after the coating deposition under various pressure conditions in the RF MS process (Ub = 0V).

Optimisation of the deposition process

In Table 2, the summarisation in relation to the de-position conditions as well as the H_{IT}, E_{IT} and COF results can be seen. Besides the target coil current of 1.5 A, the power supply on target of 50 W (samples no. 1 ÷ 5) and 100 W (samples no. 6 ÷ 8) and the current intensity of 1.57 $W \cdot cm^{-2}$ and 0.78 $W \cdot cm^{-2}$ were the additional parameters, which were used in the deposition process. Moreover, the time for the deposition was 240 minutes and the coating thickness was no more than 1.0 µm. Based on the optimisation of the deposition pressure as well as the bias of the RF MS, sample no. 7 exhibits the highest hardness (H_{IT} = 22.2 ± 1.3 GPa and E_{IT} = 271 ± 23.5 GPa). In comparison with the values of sample no. 7, sample no. 2 exhibited a decrease in hardness by only 5 %, but the COF value was equal to 0.29 and it stands for a decrease even by 65 %. The given finding above can be attributed to the

higher power supply on the target. In this case, the lower power of the magnetron coil is more effective because the COF is noticeably lower and it can be due to the higher C content in the coating, which represents the dry lubricant at the sliding friction. In the case of sample no. 5, the lowest value of hardness was determined (H_{IT} = 5.6 ± 0.9 GPa and E_{IT} = 246 ± 16.7 GPa). Moreover, sample no. 5 also noticeably shows a lower COF value in comparison with the other obtained COF values and it can be the result of the higher bias value (-400 V) in comparison with the bias of 0 V, which was used in relation to the investigation of sample no. 2.

In relation to the depositions of the WC/C coatings with the addition of gases, the parameters for the deposition referred to those obtained on the basis of the process optimisation. The given optimised parameters were used for the depositions of the WC/C coatings along with the addition of different gases. While one type of deposition was based on the usage of an N_2 additive gas, the other deposition was based on the usage of an N_2 + SiH_4 additive gas mixture. The content of SiH_4 was 1.5 %, because the SiH_4 (silane) reaction is accompanied with its flammable and even explosive behaviour. The ratio of the precursor (Ar) and additive gas (N_2 or N_2 + SiH_4) was 1:1. The obtained results of the H_{IT}, E_{IT} and COF can be seen in Table 3.

As can be seen in Table 3, N_2 caused a noticeable decrease in the H_{IT} (by 40 %), E_{IT} (by 20 %) and COF (by 65 %). A significantly lower amount of COF could be effective for low loading forces (for a low contact area pressure) in comparison with the surface with the deposited coating without the additive gases. Although a lower value of hardness could cause higher wear of the coating. On the other hand, the N_2 + SiH_4 gas mixture caused a decrease in the H_{IT} (by less than 5 %) and E_{IT} (by 10 %), but the decrease in the COF was not so notable (it was only by 25 %) and this can be effective from the aspect of wear, because the hardness can have the significant effect on the wear of the surface with the deposited coating. Based on the facts above, the N_2 + SiH_4 gas mixture can be more effective in relation to the higher loading forces.

Table 3. The results of the HIT, EIT and COF values in relation to the gas mixture composition.

Gas mixture	H_{IT} (GPa)	E_{IT} (GPa)	COF (–)
Ar	22.2 ± 1.3	271 ± 23	0.65 ± 0.10
N_2	13.5 ± 1.0	215 ± 17	0.23 ± 0.02
N_2 + SiH_4	21.9 ± 1.1	238 ± 19	0.48 ± 0.07

Influence of the annealing temperature and various gas mixtures

Ar effect

In relation to the morphology at the RT after the Ar effect, the structure of the tested samples was smooth grained with a columnar character and the size of the particles was up to 50 nm. After the annealing process at 500 °C, the areas with the clusters of the coating were observed (Figure 2b). Moreover, the given areas in a size from 0.5 μm up to 1.2 μm exhibited a smooth grained structure. The annealing process at 800 °C revealed the mutual joining of the areas with the clusters and it can be related to the formation of a continual or compact distribution of the coating on the substrate, but there was also the occurrence of areas without the coating (Figure 2c). The areas without the coating are recognisable even at low resolution.

The phase analysis (Figure 3) at the RT revealed the presence of WC_{1-x} (ICDD ref. code: 00-020-1316) as well as WO_3 phases (ICDD ref. code: 00-020-1323). The significant influence of the annealing process on the phase composition was not observed, because there was only slight increase in the intensity of carbidic and oxidic maximum.

Based on the determination of the mechanical properties with GDOES, the thickness of the evaluated coating after the deposition was about 0.7 μm (Figure 2d). The H_{IT} of the coating (Figure 4a) was 22.5 GPa before annealing and this value was closer to the maximum value [14, 16], the minimum value [15] and the average value [19]. With regard to the C content on the surface of the WC/C coating (Figure 2d), the measured hardness

Table 2. The technological parameters applied during the RF MS process with the mechanical and tribological properties of the investigated WC/C coatings.

Sample no.	Power on target (W)	Pressure (Pa)	Bias (-V)	Current (A)	H_{IT} (GPa)	E_{IT} (GPa)	COF (–)
1	50	2	0	0	8.4 ± 0.7	135 ± 9.2	0.70
2		1			21.6 ± 1.4	248 ± 18.6	0.29
3		1	340	0.1	6.8 ± 0.3	245 ± 10	0.68
4		2			6.4 ± 0.5	298 ± 14.9	0.57
5		1	400	0.05	5.6 ± 0.9	246 ± 16.7	0.39
6	100	0.8	0	0	17.1 ± 1.1	266 ± 13.4	0.96
7		1.2			22.2 ± 1.3	271 ± 23.5	0.82
8		1.5			19.4 ± 1.8	240 ± 20.9	0.60
9		1			14.5 ± 0.5	185 ± 5.2	0.90
10		1			19.4 ± 0.2	294 ± 7.1	0.77

is in agreement with the review published by Mrabet et *al.* in [18]. It can also be concluded that the measured value of H_{IT} is close to [18] but the C content is lower (≈ 25.6 % [18]). The C content in our coating is ≈ 30.0 wt. % (Figure 2d).

The heat treatment of the sample at 200 °C led to a negligible decrease in the hardness, whereas during annealing at 500 °C, there was a decrease in the hardness under 13 GPa. On the other hand, the slight increase in hardness to the value of 15 GPa was observed after annealing at 800 °C. Relating to the COF of the WC/C coating before annealing, the value was equal to 0.36 (sample no. 5) and 0.29 (sample no. 2). While it is close to and even lower than the maximum value in [10], it is three or even four times higher than the value presented in [8] as well as two times lower than the minimum value presented in [17, 18]. The values of the COF (Figure 4b) had a similar character, considering the hardness course. At the RT, there was a decrease in the COF from the maximum value of 0.38 to the minimum value under 0.2 after annealing at 500 °C, but after annealing at 800 °C, there was an increase in the COF value, which was 0.29. The measured average value of the COF at the RT corresponds with [18] although the wt. % of C in the coating is 10 %, while, in the evaluated WC/C coating, the content of C is 41 % (Figure 2d).

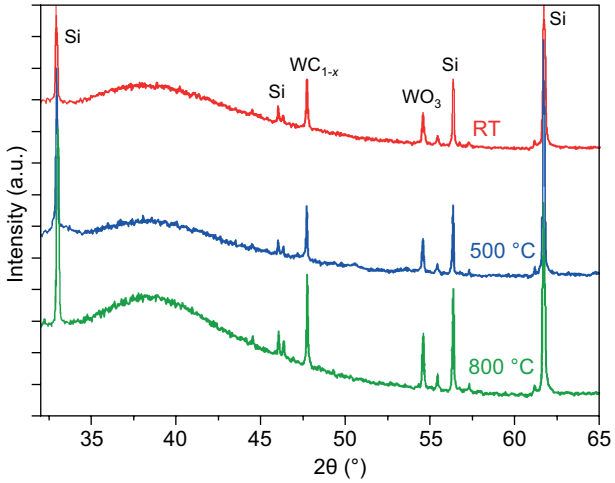

Figure 3. The XRD of the WC/C coatings before annealing (RT) and after annealing at 500 °C and 800 °C.

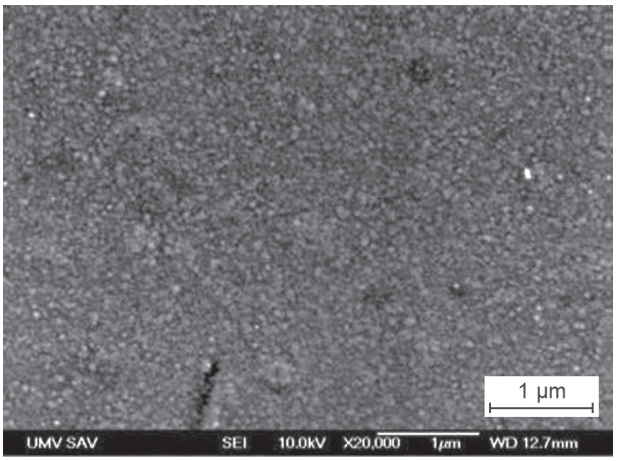

a)

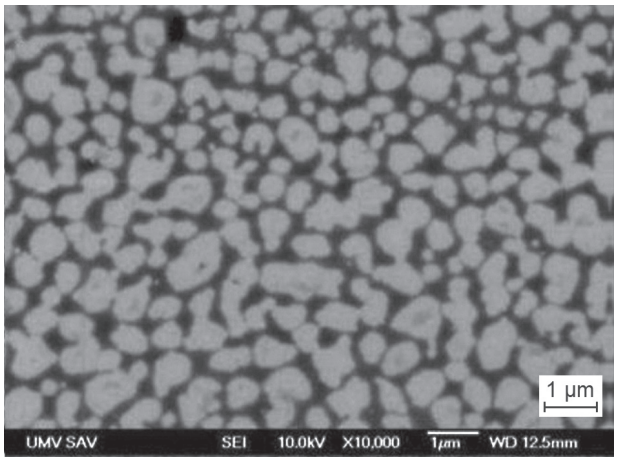

b)

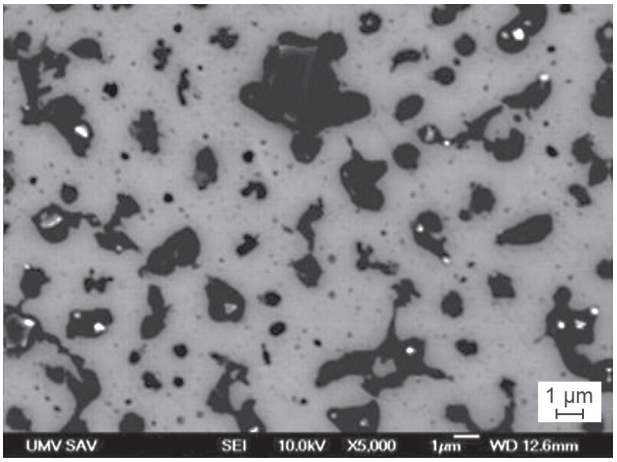

c)

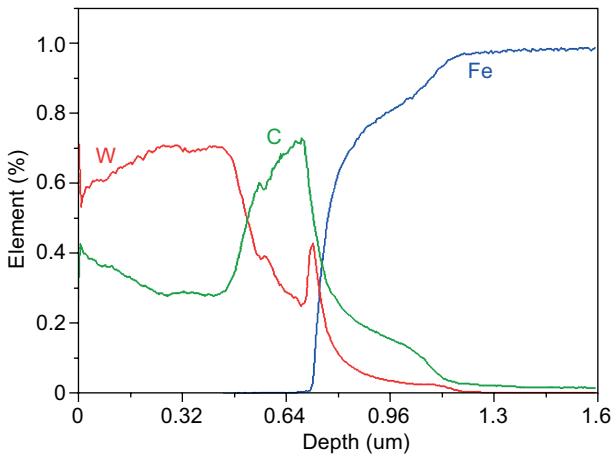

d)

Figure 2. The surface morphology of the WC/C coatings (SEM): a) before annealing; b) after annealing at 500 °C; c) after annealing at 800 °C; d) cross sectional chemical composition of the WC/C coating before annealing (GDOES).

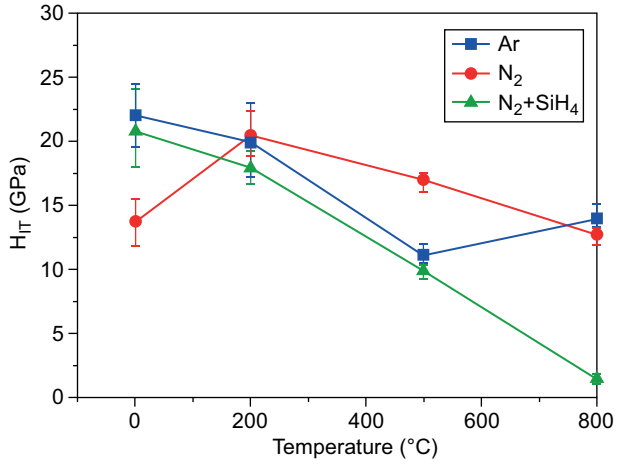

a)

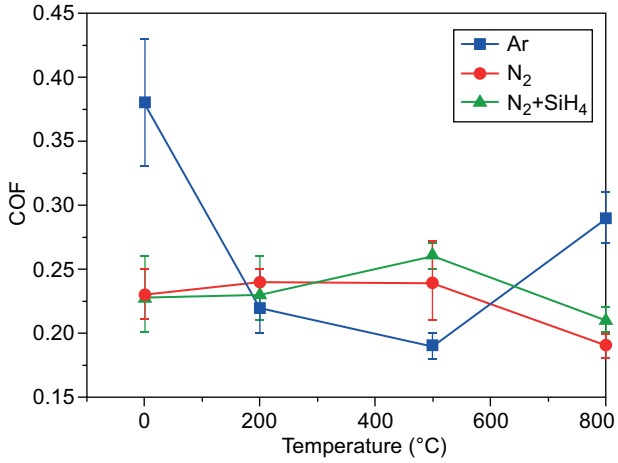

b)

Figure 4. Dependence of H_{IT} (a) and COF (b) on the annealing temperature of the WC/C coatings with and without the additive gases.

N_2 effect

As can be seen in Figure 5, the coating surface was smooth grained without any significant recognisable structure features at low as well as high resolutions. A slight change was observed after annealing at 500 °C, because there was the indication of columns on the sample surface (Figure 5b). The annealing process at 800 °C led to the start of the alteration of the coating's surface (Figure 5c - Areas, where the swelling process starts are marked with arrows) due to exposure of the coating surface to O_2 and the subsequent reaction of O_2 with C, resulting in the formation of CO_2, which was released from the coating surface and it caused the start of the swelling process as is described in [32].

The phase analysis of the WC/C coating (Figure 6),which was deposited along with the reactive N_2 additive gas, exhibits a similar character, compared with the Ar effect. The presence of WC_{1-x} (ICDD ref. code: 00-020-1316) as well as WO_3 phases (ICDD ref. code: 00-020-1323) was recognised in the structure. The significant influence of the annealing process on the phase composition was not observed. There was only a slight increase in the intensity of the carbidic and oxidic minimum.

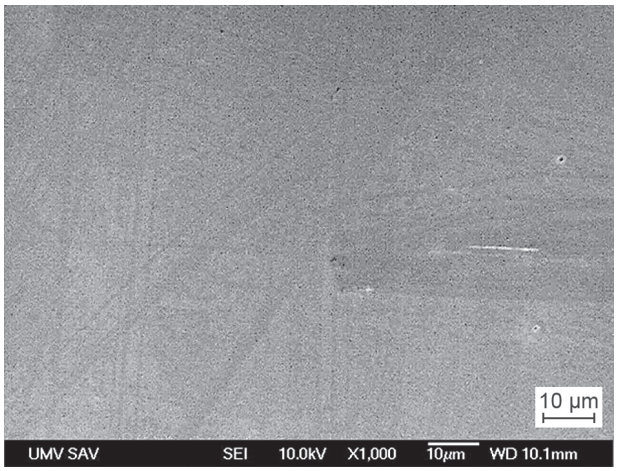

a)

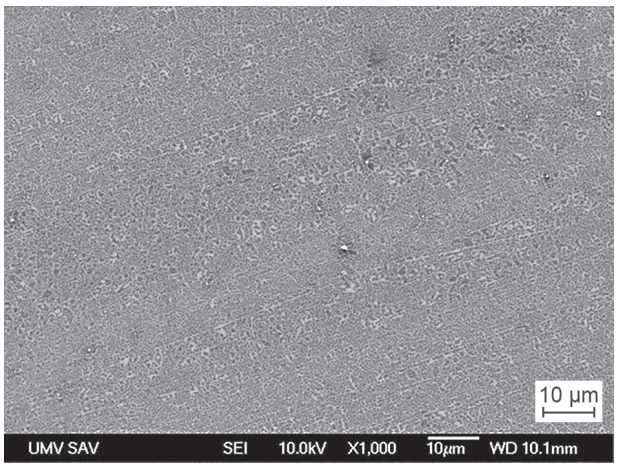

b)

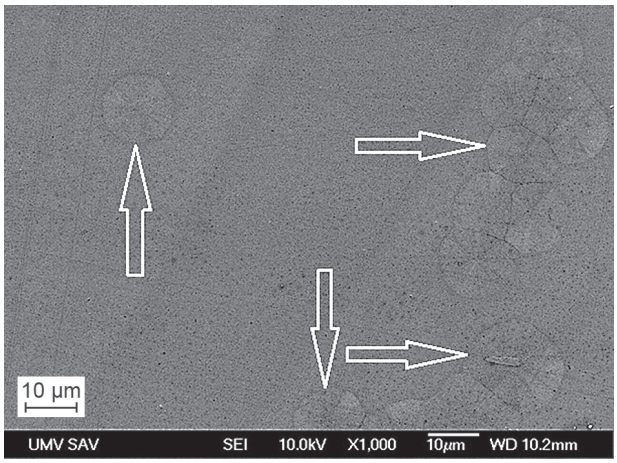

c)

Figure 5. The surface morphology of the WC/C coatings (SEM) with N_2: a) before annealing, after annealing at: b) 500 °C, c) 800°C (areas, where the swelling process starts are marked with arrows). *(Continue on next page)*

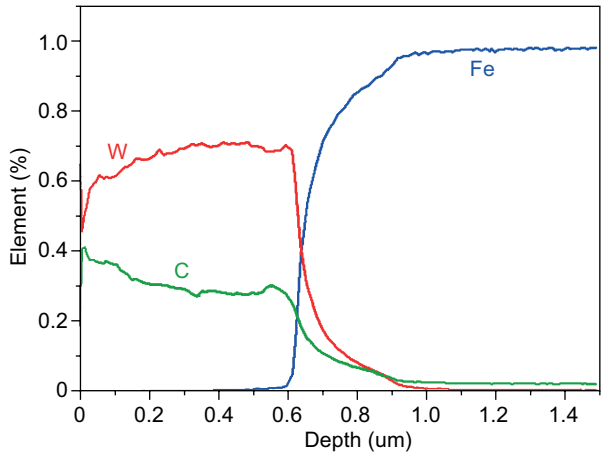

d)

Figure 5. d) Cross sectional chemical composition of the WC/C coating before annealing (GDOES).

In comparison with the layers which were deposited without any additive gases (Figure 4a), the WC/C coating with the N_2 additive gas exhibits a noticeable lower hardness before the annealing process. The H_{IT} value is less than 14 GPa and it is less by 35 % in comparison with the value standing for the coatings, which were deposited without any additive gasses. The H_{IT} value we measured is lowered by 50 % in comparison with [23]. That can be caused by the absence of the W_2N phase in the measured coating. After annealing at 500 °C, there was an increase in the hardness to value of 17 GPa. A further annealing process at 800 °C led to a decrease in the hardness to the value of 15 GPa, but it is more than the value of 14 GPa at the RT. At the RT as well as after annealing at 500 °C, the COF exhibits the same value, which is 0.23. The performance of the annealing process at 800 °C caused the decrease in the COF to the value of 0.2. The behaviour of the H_{IT} and COF values (at the RT and after annealing at 200 °C and 500 °C) was

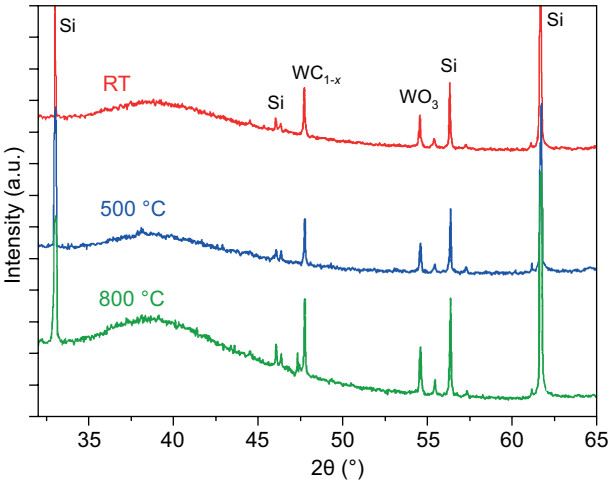

Figure 6. The XRD of the WC/C coatings with N2 before annealing (RT) and after annealing at 500 °C and 800 °C; the Si phase (ICDD ref. code: 00-027-1402).

similar to [4]. We can state that the average value of the COF measured by us at the RT is 30 % lower compared to the minimal COF value, which was measured in [23]. Concerning the absence of a hard W_2N phase, the presence of C is partially serving as a lubricant, which can be the cause of the lowered COF value.

The N_2 and SiH_4 effect

In the case of the morphology evaluation (Figure 7), the surface of the WC/C coating exhibited a smooth grained columnar structure with a column thickness up to 50 nm at the RT. After annealing at 500 °C, there was the occurrence of empty areas with the width from 100 up to 600 nm (Figure 7b – see arrows). The given empty areas can be attributed to the oxidation process leading to the formation of WO_3 oxides (ICDD ref. code: 00-020-1323) and the WC_{1-X} carbide phase (ICDD ref. code: 00-020-1316). We can presume that the partial pressure of SiH_4 lowers by adding N_2 (with a constant total pressure in the vacuum chamber), then the amount of Si in the coating lowers at the expense of N_2. This can lead to a decrease of corrosion resistance and refractoriness. The annealing process at 800 °C led to a coating rupture due to exposure of the coating surface to O_2 and the subsequent reaction of O_2 with C, resulting in the formation of CO_2, which was released from the coating surface and it caused the swelling process as is seen in [32]. The columnar character of the coating was not more recognisable and there were cracks on the coating surface (Figure 7c – see arrows), which are also described in [31].

Relating to the structure analysis (Figure 8), the presence of an amorphous structure was based on the phase evaluation of the coating at the RT. After annealing at 500 °C, the presence of WC_{1-x} (ICDD ref. code: 00-020-1316) as well as the WO_3 phases (ICDD ref. code: 00-020-1323) was observed in the structure. The coating was amorphous, but there was the tendency to form nanocrystals. There was not any change of the coating structure after a further annealing process at 800 °C. The decrease in the maxima of the WC_{1-x} phase (ICDD ref. code: 00-020-1316) and the WO_3 oxide (ICDD ref. code: 00-020-1316) were observed only.

Based on the determination of the mechanical properties (Figure 4) with GDOES, the thickness of the evaluated coating after the deposition was about 0.7 µm (Figure 7d). The H_{IT} was equal to 22 GPa at the RT and is the same as [28]. The given value is comparable to the value of the coating, which was deposited in the Ar environment. The H_{IT} values were comparable to values standing for the coating without the N_2 additive gas (deposited only with Ar) under the temperature of 500 °C. After annealing at 500 °C, there was a decrease in the H_{IT} to value of 12 GPa and further annealing at 800 °C led to a decrease in the H_{IT} again, while the value of the H_{IT} was under 5 GPa. This decrease in the H_{IT} is caused by the strong decomposition of the evaluated

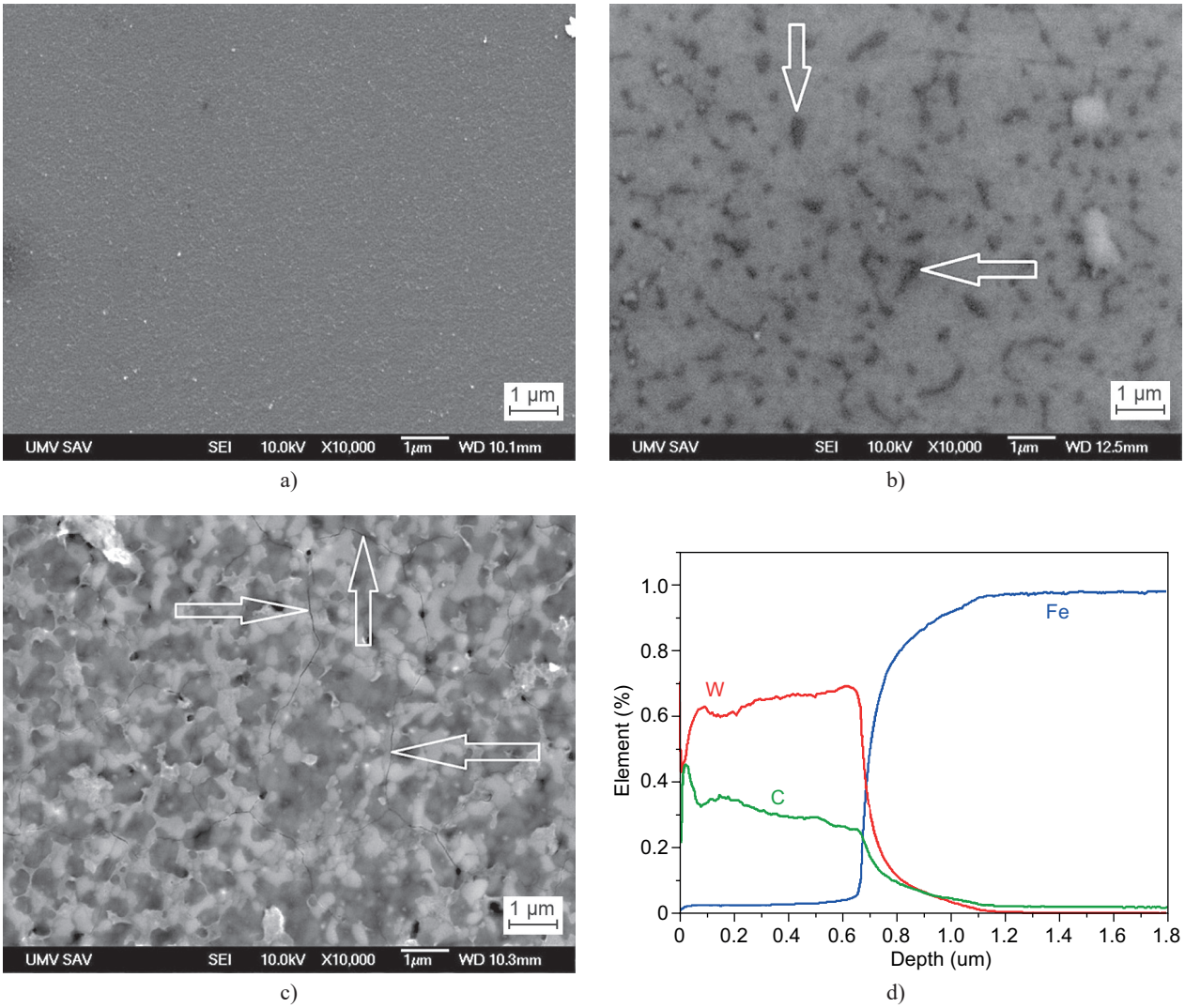

Figure 7. The surface morphology of the WC/C coatings (SEM) with N2+SiH4: a) before annealing, after annealing at: b) 500 °C (empty areas are signed by arrows), c) 800 °C (cracks are signed by arrows) and d) cross sectional chemical composition of the WC/C coating before annealing (GDOES).

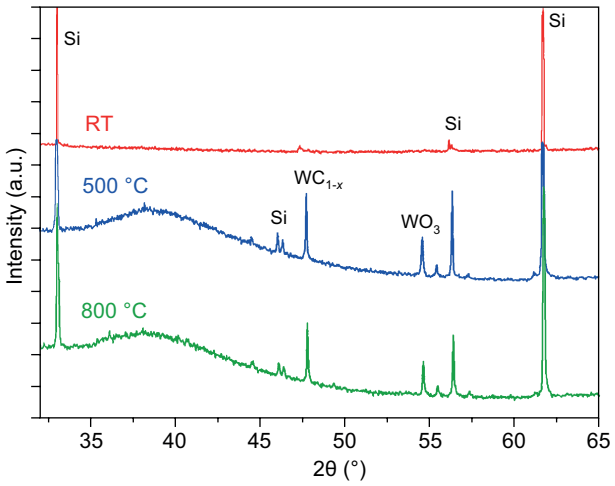

Figure 8. The XRD of the WC/C coatings with N_2+SiH_4: before annealing (RT) and after annealing at 500 °C and 800 °C.

coating (Figures 7b, 7c) as a result of the oxidation reaction of O with C and the subsequent swelling of the coating mentioned above. Relating to the COFs, the values, as the representatives of the course, were close to the COF values of the coating with the N_2 additive gas. The COF values are in the range (interval) from 0.23 up to 0.25 at RT as well as after annealing at 500 °C, but after annealing at 800 °C, there was a decrease in the COF to the value of 0.22.

CONCLUSIONS

On the basis of the performed experiments, we can draw the following conclusions:

- By optimising the process of the deposition, the WC/C coating was prepared with maximal hardness

(22.2 ± 1.3 GPa) using the pressure equal to 1.2 Pa and a negative bias (U_b) of the sample holder equal to 0 V. On other hand, the values of COF were equal to 0.65 ± 0.10.

Adding N_2 in the deposition process causes (before annealing) a significant decrease in the H_{IT}, E_{IT} and COF of the WC coating when compared to the coating deposited without the mentioned gases. On the other hand, the gas mixture N_2 + SiH_4 caused a significant decline in the COF only.

- After the annealing process at 200 °C, there was a decrease in the H_{IT} of the WC/C coating, which was deposited without any additive gas as well as with the N_2 additive gas. Furthermore, the N_2 + SiH_4 gas mixture caused an increase in the H_{IT} of the WC/C coating up to the value which was close to the H_{IT} of the WC/C coating, which was deposited without any additive gas. The COF was from 0.2 up to 0.23 after the given annealing process.
- The added N_2 significantly enhances the refractoriness (especially at 800 °C) in comparison to the coating deposited without the mentioned gases. On the other hand, the gas mixture N_2 + SiH_4 markedly reduces their refractoriness. It is evident due to the decomposition of the WC/C coating (based on the observation of the morphology).
- The coating degradation was accompanied by the swelling of the coating.
- In comparison with the N_2 + SiH_4 gas mixture, N_2 (as an additive gas) is more effective for temperatures under 800 °C, because it has a better effect from the aspect of avoiding the WC/C coating decomposition.

Acknowledgements

This work was financially supported by the Slovak Grant Agency under the grants VEGA 1/0432/17, 1/0708/16 and 1/0219/18. It is also the result of the projects APVV-16-0359, APVV-17-0258 and KEGA 030TUKE-4/2017.

REFERENCES

1. Deng X., Cleveland C., Karcher T., Koopman M., Chawla N., Chawla K.K. (2005): Nanoindentation behavior of nanolayered metal-ceramic composites, *Journal of Materials Engineering and Performance*. 14 (4), 417-423. doi: 10.1361/105994905X56115
2. Zhao H., Mu Ch., Ye F. (2016): Microtribological mechanisms of tungsten and aluminum nitride films, *Journal of Materials Engineering and Performance,* 25 (4), 1446-1452. doi: 10.1007/s11665-016-2008-5
3. Drábik M., Truchlý M., Ballo V., Roch T., Kvetková L., Kúš P. (2018): Influence of substrate material and its plasma pretreatment on adhesion and properties of WC/a-C:H nanocomposite coatings deposited at low temperature, *Surface Coatings and Technology*, 333, 138–147. doi: 10.1016/j.surfcoat.2017.10.081
4. Horňák P.. Kottfer D., Kaczmarek L., Kianicová M., Balko J., Rehák F., Pekarčíková M., Čižnár P. (2018): The effect of pressure, bias voltage and annealing temperature on N_2 and N_2+SiH_4 doped WC/C DC magnetron sputtered layers, *Ceramics-Silikaty*, 62(1), 97-107. doi: 10.13168/cs.2018.0001
5. Rebholz C., Schneider J.M., Ziegele H., Rähle B., Leyland A., Matthews A. (1998): Deposition and characterisation of carbon-containing tungsten layers prepared by reactive magnetron sputtering, *Vacuum,* 49(4) 265-272. doi: 10.1016/S0042-207X(98)00122-5
6. Rebholz C., Schneider J.M., Leyland A., Matthews A. (1999): Wear behaviour of carbon-containing tungsten layers prepared by reactive magnetron sputtering, *Surface Coatings and Technology*, 112, 85–90. doi: 10.1016/S0257-8972(98)00786-5
7. Wänstrand O., Larsson M., Hedenqvist P. (1999): Mechanical and tribological evaluation of PVD WC/C layers, *Surface Coatings and Technology*, 111, 247–254. doi: 10.1016/S0257-8972(98)00821-4
8. Agudelo-Morimitsu L.C., DeLaRoche J., Escobar D., Ospina R., Restrepo-Parra E. (2013): Substrate heating and post-annealing effect on tungsten/tungsten carbide bilayers grown by non-reactive DC magnetron sputtering, *Ceramics Interntional,* 39, 7355–7365. doi: 10.1016/j.ceramint.2013.02.075
9. Agudelo-Morimitsu L.C., DeLaRoche J., Ruden A., Escobar D., Restrepo-Parra E. (2014): Effect of substrate temperature on the mechanical and tribological properties of W/WC produced by DC magnetron sputtering, *Ceramics Interntional,* 40, 7037–7042. doi: 10.1016/j.ceramint.2013.12.033
10. Sánchez-López J.C., Martínez-Martínez D., Abad M.D., Fernández A. (2009): Metal carbide/amorphous C-based nanocomposite layers for tribological applications, *Surface Coatings and Technology*, 204, 947–954. doi: 10.1016/j.surfcoat.2009.05.038
11. Zhou S., Wang L., Wang S.C., Xue Q. (2011): Comparative study of simplex doped nc-WC/a-C and duplex doped nc-WC/a-C(Al) nanocomposite coatings, *Applied Surface Science,* 257, 6971–6979. doi: 10.1016/j.apsusc.2011.03.045
12. Baragetti S., Gerosa R., Rivolta B., Silva G., Tordini F. (2011): Fatigue behavior of foreign object damaged 7075 heat treated aluminum alloy coated with PVD WC/C, *Procedia Engineering,* 10, 3375–3380. doi: 10.1016/j.proeng.2011.04.556
13. Vera E.E., Vite M., Lewis R., Gallardo E.A., Laguna-Camacho J.R. (2011): A study of the wear performance of TiN, CrN and WC/C coatings on different steel substrates, *Wear,* 271, 2116–2124. doi: 10.1016/j.wear.2010.12.061
14. Abdelouahdi K., Sant C., Legrand-Buscema C., Aubert P., Perrière J., Renou G., Houdy Ph. (2006): Microstructural and mechanical investigations of tungsten carbide films deposited by reactive RF sputtering, *Surface Coatings and Technology*, 200, 6469–6473. doi: 10.1016/j.surfcoat.2005.11.015
15. Esteve J., Zambrano G., Rincon C., Martinez E., Galindo H., Prieto P. (2000): Mechanical and tribological properties of tungsten carbide sputtered layers, *Thin Solid Films*, 373, 282-286. doi: 10.1016/S0040-6090(00)01108-1

16. Rincón C., Romero J., Esteve J., Martíinez E., Lousa A. (2003): Effects of carbon incorporation in tungsten carbide films deposited by r.f. magnetron sputtering: single layers and multilayers, *Surface Coatings and Technology,* 163–164, 386–391. doi: 10.1016/S0257-8972(02)00635-7
17. Abad M.D., Muñoz-Márquez M.A., El Mrabet S., Justo A., Sánchez-López J.C. (2010): Tailored synthesis of nanostructured WC/a-C layers by dual magnetron sputtering, *Surface Coatings and Technology,* 204, 3490–3500. doi: 10.1016/j.surfcoat.2010.04.019
18. El Mrabet S., Abad M.D., Sánchez-López J.C. (2011): Identification of the wear mechanism on WC/C nanostructured coatings, *Surface Coatings and Technol*ogy, 206, 1913–1920. doi: 10.1016/j.surfcoat.2011.07.059
19. Czyzniewski A. (2003): Deposition and some properties oo nanocrystalline WC and nanocomposite WC/a-C:H coatings, *Thin Solid Films*, 433, 180–185. doi: 10.1016/S0040-6090(03)00324-9
20. Makowka M., Pawlak W., Konarski P., Wendler B. (2016): Hydrogen content influence on tribological properties of nc-WC/a-C:H coatings, *Diamond and Related Materials,* 67, 16–25. doi: 10.1016/j.diamond.2016.01.007
21. Park Y. S., Park Y., Jung H., Jung T.-H., Lim D.-G., Choi W. S. (2012): Tribological properties of a-C:W film deposited by radio frequency magnetron Co-sputtering method, *Thin Solid Films*, 521, 107–111. doi: 10.1016/j.tsf.2012.02.042
22. Li Y., Zhang A., Li G. (2015): The influence of microstructure on mechanical property of polytypic TiC/WC nanomultilayers, *Vacuum,* 117, 23-26. doi: 10.1016/j.vacuum.2015.03.027
23. Zhao H., Ni Z., Ye F. (2016): Effect of carbon content on structure and properties of WCN coatings prepared by RF magnetron sputtering, *Surface Coatings and Technol*ogy, 287, 129–137. doi: 10.1016/j.surfcoat.2016.01.003
24. Moura e Silva C.W., Branco J.R.T., Cavaleiro A. (2006): Characterization of magnetron co-sputtered W-doped C-based films, *Thin Solid Films,* 515, 1063–1068. doi: 10.1016/j.tsf.2006.07.084
25. Sun Y.-M., Lee S.Y., Lemonds A.M., Engbrecht E.R., Veldman S., Lozano J., White J.M., Ekerdt J.G., Emesh I., Pfeifer K. (2001): Low temperature chemical vapor deposition of tungsten carbide for copper diffusion barriers, *Thin Solid Films,* 397, 109-115. doi: 10.1016/S0040-6090(01)01367-0
26. Ferdinandy M., Lofaj F., Dusza J., Kottfer D. (2011): Preparation of Nanocrystalline WC Layers by Plasma Enhanced CVD-PVD Employing $W(CO)_6$ decomposition (in slovak). *Chemické listy – Chemical letters*, 105, 442 – 444.
27. Lofaj F., Ferdinandy M., Kottfer D., Dusza J., Němeček J. (2009): Tribological Properties of the Cr–C and W–C Based PECVD Nanocomposite Layers, in: Proceedings of the 11th ECERS Conference, Krakow.
28 Lofaj F., Ferdinandy M., Horňak P. (2014): Nanohardness vs. Friction behavior in magnetron sputtered and PECVD W-C coatings, *Key Engineering Materials,* 586, 35-38. doi: 10.4028/www.scientific.net/KEM.586.35
29. Horňak P. (2016). *The influence of deposition technology on selected properties of WC–C layers.* PhD. Thesis (in slovak), Alexander Dubček University of Trenčín, p. 104.
30. Lofaj F., Kvetková L., Hviščová P., Gregor M., Ferdinandy M. (2016): Reactive processes in the high target utilization sputtering (HiTUS) W–C based coatings, *Journal of European Ceramic Society,* 36, 3029–3040. doi: 10.1016/j.jeurceramsoc.2015.12.043
31. Toby B.H. (2005): CMPR – a powder diffraction toolkit, *Journal of Applied Crystallography*, 38, 1040-1041. doi: 10.1107/S0021889805030232
32. Lofaj F., Kaganowskyy Yu.S. (1995): Kinetics of WC–Co oxidation accompanied by swelling, *Journal of Material Science,* 30, 1811-1817. doi: 10.1007/BF00351615